

See discussions, stats, and author profiles for this publication at: <https://www.researchgate.net/publication/281339883>

# Evidence for Hydroxamate Siderophores and Other N-Containing Organic Compounds Controlling $^{239,240}\text{Pu}$ Immobilization and Remobilization in a Wetland Sediment

ARTICLE *in* ENVIRONMENTAL SCIENCE & TECHNOLOGY · AUGUST 2015

Impact Factor: 5.33 · DOI: 10.1021/acs.est.5b02310 · Source: PubMed

CITATION

1

READS

180

## 11 AUTHORS, INCLUDING:



**Chen Xu**

Texas A&M University

60 PUBLICATIONS 820 CITATIONS

SEE PROFILE



**Saijin Zhang**

Texas A&M University - Galveston

54 PUBLICATIONS 714 CITATIONS

SEE PROFILE



**Daniel I. Kaplan**

Savannah River National Laboratory

220 PUBLICATIONS 2,661 CITATIONS

SEE PROFILE



**Kathleen A Schwehr**

Texas A&M University - Galveston

40 PUBLICATIONS 703 CITATIONS

SEE PROFILE

## Evidence for Hydroxamate Siderophores and Other N-Containing Organic Compounds Controlling <sup>239,240</sup>Pu Immobilization and Remobilization in a Wetland Sediment

Chen Xu,<sup>\*,†</sup> Saijin Zhang,<sup>†</sup> Daniel I. Kaplan,<sup>‡</sup> Yi-Fang Ho,<sup>†</sup> Kathleen A. Schwehr,<sup>†</sup> Kimberly A. Roberts,<sup>‡</sup> Hongmei Chen,<sup>§</sup> Nicole Didonato,<sup>§</sup> Matthew Athon,<sup>†</sup> Patrick G. Hatcher,<sup>§</sup> and Peter H. Santschi<sup>†</sup>

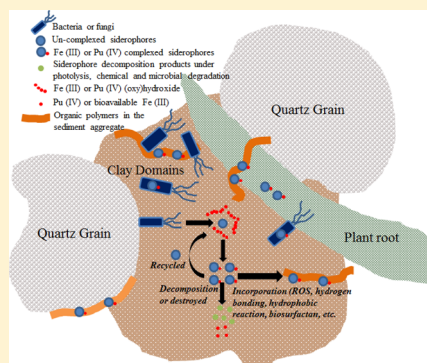
<sup>†</sup>Department of Marine Sciences, Texas A&M University, Building 3029, Galveston, Texas 77553, United States

<sup>‡</sup>Savannah River National Laboratory, Aiken, South Carolina 29808, United States

<sup>§</sup>Department of Chemistry and Biochemistry, College of Sciences, Old Dominion University, Norfolk, Virginia 23529, United States

**S** Supporting Information

**ABSTRACT:** Pu concentrations in wetland surface sediments collected downstream of a former nuclear processing facility in F-Area of the Savannah River Site (SRS), USA, were ~2.5 times greater than those measured in the associated upland aquifer sediments; similarly, the Pu concentration solid/water ratios were orders of magnitude greater in the wetland than in the low-organic matter content aquifer soils. Sediment Pu concentrations were correlated to total organic carbon and total nitrogen contents and even more strongly to hydroxamate siderophore (HS) concentrations. The HS were detected in the particulate or colloidal phases of the sediments but not in the low molecular fractions (<1000 Da). Macromolecules which scavenged the majority of the potentially mobile Pu were further separated from the bulk mobile organic matter fraction ("water extract") via an isoelectric focusing experiment (IEF). An electrospray ionization Fourier-transform ion cyclotron resonance ultrahigh resolution mass spectrometry (ESI FTICR-MS) spectral comparison of the IEF extract and a siderophore standard (desferrioxamine; DFO) suggested the presence of HS functionalities in the IEF extract. This study suggests that while HS are a very minor component in the sediment particulate/colloidal fractions, their concentrations greatly exceed those of ambient Pu, and HS may play an especially important role in Pu immobilization/remobilization in wetland sediments.



## INTRODUCTION

Wetlands usually act as a buffering zone and sink for many contaminants, such as pesticides,<sup>1–3</sup> trace metals,<sup>4</sup> and actinides.<sup>5</sup> However, in some unexpected cases, they can emerge as contaminant sources to downstream ecosystems. For example, by transferring from Al–P–Fe–Si aggregates in the wetland sediment and binding to the Fe–organic matter colloids in the porewater, U(IV), which was conventionally regarded as immobile, was highly mobile and released from the wetland into the streamwater.<sup>6</sup> In another study, Xu et al.<sup>7</sup> documented a pH-driven immobilization and remobilization scheme for colloidal organic matter associated Pu. Mobility of Pu(IV) increased when pH increased due to (1) a greater desorption of sediment organic matter as colloidal organic matter under alkaline conditions as a result of enhanced solubility of organic macromolecules at higher pH and (2) Pu(IV) preferentially binding to this colloidal organic matter carrier rather than the immobile sedimentary organic matter. Furthermore, the influence of oxidation state (Pu(IV) vs Pu(V)) on Pu mobility in an organic-rich wetland area was the opposite of that in low organic sediments. Pu(IV) is more mobile than Pu(V) in high-organic matter soils because of the much stronger tendency for Pu(IV) to bind to the mobile

colloidal organic matter. Conversely, in low-organic matter soils, the Pu(IV) binds appreciably more strongly to the sediment than Pu(V). However, the Pu(V) eventually binds to the mineral soils after undergoing reduction.<sup>8–11</sup>

The Savannah River Site (SRS), located along the Savannah River in South Carolina, encompasses roughly 830 km<sup>2</sup>, one-fifth of which is designated as wetlands. Most of the wetlands and dense wetland forests on this secure site have had minimal anthropogenic disturbance over the last 60 years. The SRS produced ~40 t of Pu, one-third of the nation's inventory between 1954 and 1989, for nuclear material production mostly for defense purposes but also for fuels for submarines and medical, industrial, and scientific applications. As a consequence, F-Area unlined earthen disposal basins, or seepage basins, of the SRS received waste effluents containing a total of 444 GBq (12 Ci) of <sup>239</sup>Pu over the years through direct disposal.<sup>12</sup> Groundwater flowing southeast from the seepage basins toward Fourmile Branch, a second-order stream and

Received: May 8, 2015

Revised: August 25, 2015

Accepted: August 27, 2015



tributary of the Savannah River (Figure S1),<sup>13</sup> has transported Pu into downstream wetlands, resulting in  $5 \times 10^{-238}\text{Pu}$  and  $7 \times 10^{-239,240}\text{Pu}$  concentrations in the wetland sediments compared to upland sediments northern to the seepage basin that were not in the plume path and thus minimally impacted by contamination.<sup>14</sup>

The human and environmental risks associated with Pu disposal and remediation scenarios mainly stem from the radioactivity and the very long half-lives for several isotopes. The ratios of  $^{240}\text{Pu}/^{239}\text{Pu}$  can be used to trace the specific Pu source. Global fallout has an average  $^{240}\text{Pu}/^{239}\text{Pu}$  ratio of 0.18. Weapons-grade Pu is characterized by a low content of  $^{240}\text{Pu}$  and thus a low  $^{240}\text{Pu}/^{239}\text{Pu} < 0.07$ .<sup>15</sup> In addition, source-dependent (*in situ* decay of progenitor radionuclide such as  $^{244}\text{Cm}$ ) and source-independent (pH, redox potential/state/condition, and association with colloids) factors also regulate Pu isotope concentrations and geochemical behavior.<sup>7,13</sup>

Colloidal organic matter has been identified as an important vector for remobilizing Pu in SRS wetland sediments,<sup>7</sup> which contains abundant organic carbon (8–24 wt %).<sup>16–19</sup> However, the molecular characteristics of this Pu carrier, which was extracted from a wetland representing a warm and humid climate, have not been reported. Colloidal organic macromolecules, recovered through ultrafiltration and isoelectric focusing electrophoresis (IEF) from contaminated soils in Rocky Flats Environment and Technology Site (RFETS, Colorado, USA), were determined to be specifically responsible for scavenging  $\geq 80\%$  of the total Pu remobilized into streams during storm runoffs, pond discharge, and wind dispersion events.<sup>20,21</sup> This Pu vector was shown, using spectrophotometric methods, to contain hydroxamates (a class of organic compounds bearing CONOH chelating groups) and was enriched in N. By a combination of  $^1\text{H}$  NMR,  $^{13}\text{C}$  NMR, and 2-D  $^1\text{H}$ – $^{13}\text{C}$  and  $^1\text{H}$ – $^1\text{H}$  NMR (HSQC and COSY), it was further characterized as a cutin degradation product cross-linked to hydrophilic moieties (e.g., polysaccharides), with a conformation that rendered it mobile in the surface sediment. However, molecular-level characterization of the actual Pu binding sites within this Pu vector was not accomplished.<sup>22</sup>

A few studies have discussed the role of soil-bound siderophore compounds with regards to contaminant complexation and soil/water partitioning.<sup>22–24</sup> This study focuses on unraveling the molecular information on the naturally present biogeopolymers that are capable of immobilizing or remobilizing Pu in wetland environments. Specifically, the objectives of this study were: (1) to determine the siderophore concentrations and distributions in the wetland sediments; (2) to measure wetland sediment Pu concentrations and isotopic ratios ( $^{240}\text{Pu}/^{239}\text{Pu}$ ) and correlate the concentrations of hydroxamate siderophores (HS) with Pu concentrations; (3) to isolate Pu-enriched macromolecules from the colloidal fraction of the sediment aggregates by a recently established method, followed by characterization using electrospray ionization Fourier-transform ion cyclotron resonance ultrahigh resolution mass spectrometry (ESI FTICR-MS). The advantage of ESI-FTICRMS over other molecular-level analytical techniques such as GC-MS or HPLC-MS is that it provides detailed molecular-level information on the intact macromolecules within natural organic matter (NOM),<sup>25,26</sup> without previous derivatization, or gas- or liquid-chromatography separation. Less sample is needed (in the scale of  $\mu\text{g}$  C or N), compared to NMR (usually in the scale of mg C or N). Molecular formula can be assigned accurately, due to its ultrahigh resolution. The

general approach was designed to enable us to study Pu and NOM interactions at environmentally relevant Pu concentrations ( $10^{-14}$  M). At elevated Pu concentrations, Pu tends to form polymeric or colloidal Pu-oxide particles (i.e., intrinsic colloids), and Pu binding behavior (e.g., sorption rate, surface-mediated reduction rate, the limited binding sites, etc.) to NOM moieties might differ greatly from that at environmentally relevant Pu concentrations.<sup>27</sup> However, direct detection of Pu to NOM moieties is not yet possible at environmentally relevant Pu concentration. Consequently, we relied on an indirect approach involving correlating sedimentary organic moieties contents with Pu concentrations, as well as a direct approach by selectively extracting Pu-enriched NOM moieties and characterizing them at molecular-level with ESI FTICR-MS.

## MATERIALS AND METHODS

**Sampling.** Four 35 to 40 cm sediment cores (FSP1, FSP2, FSP3, and FSP4) were collected with a hand auger within the contaminated wetland region of F-Area in April of 2010 (Figure S1). A fifth sediment core (FSP0) was collected within the same wetland but outside the impacted area in September of 2012 (Figure S1). A sixth sediment core (FSI18) was collected near FSP3 in September of 2008 and has been well-characterized in previous studies.<sup>7,16,28–30</sup> This core was used to obtain the mobile Pu-carrying macromolecules (soil characterization data is provided in Table S1). All sediment samples were stored and shipped in zip lock bags under ice. Once at the Texas A&M-Galveston lab, they were immediately transferred to a 4 °C refrigerator. Oven-dried sediments (50–60 °C) were homogenized, and the <2 mm sieved fraction was used for subsequent experiments, including hydroxamate determination, and elemental and Pu analysis. For extracting Pu-carrying colloidal organic matter, moist field soil was directly sieved through a 2 mm sieve to avoid possible alteration of the organic matter that might be caused by oven-drying and rewetting of the soil.<sup>31</sup>

Total elemental analysis (total carbon, nitrogen, and hydrogen) was performed with a PerkinElmer CHNS/O 2400 analyzer. Acetanilide (71.09% C, 6.71% H, and 10.36% N) was used as an analytical standard. Organic carbon content was determined after a direct acidification step using 1 N HCl.<sup>32</sup> On the basis of triplicate analyses, total carbon and organic carbon had errors well within 5%. Total  $^{239,240}\text{Pu}$  activity was measured by alpha spectrometry, and the isotopic ratios of  $^{240}\text{Pu}/^{239}\text{Pu}$  were determined by an inductively coupled plasma-mass spectrometer (ICP-MS). Details of this analytical procedure are provided in the Supporting Information.

**Particulate Hydroxamate Determination (Determination of Total Sediment Hydroxamate).** In order to maximally dissolve the mineral components, eliminate their protective support, decrease the interferences from mineral matrix, and thus release the mineral-associated organic macromolecules with the least chemical alteration, 0.5 g of sediment was pretreated overnight with 5 mL of 10% HF on an orbital shaker at 180 rpm (20 °C). This step is required, as hydroxamate siderophores (HS) are barely detected using the Csaky test<sup>33</sup> if the sediment is not pretreated with 10% HF. HF pretreatment has been found to be the most reliable and advantageous method to remove the paramagnetic species such as iron for the NMR analysis of the soil or sediment.<sup>34,35</sup> There could be some loss of dissolved hydroxamate due to digestion

**Table 1. Elemental Composition, Hydroxamate Siderophore (HS), <sup>239,240</sup>Pu Concentrations, and Pu Isotopic Ratios of the SRS F-Area Wetland Sediments<sup>a</sup>**

sampling site	depth, cm	organic carbon, wt %	total nitrogen, wt %	HS, mg-C/g-OC in sediment	HS, mg-N/g-N in sediment	<sup>239,240</sup> Pu, Bq/kg	<sup>240</sup> Pu/ <sup>239</sup> Pu	concentration solid/water ratios	
								<sup>240</sup> Pu	<sup>239</sup> Pu
FSP1	3	34.78 ± 0.13	2.26 ± 0.03	N.D	N.D	5.63 ± 0.58	N.D.	N.D.	N.D.
	8	9.50 ± 1.40	0.53 ± 0.08	N.D	N.D	11.32 ± 0.63	N.D.	N.D.	N.D.
	13	2.68 ± 0.01	0.10 ± 0.00	0.141 ± 0.020	2.20 ± 0.19	0.19 ± 0.10	N.D.	N.D.	N.D.
	18	1.52 ± 0.08	0.05 ± 0.00	0.043 ± 0.000	0.85 ± 0.00	<D.L.	N.D.	N.D.	N.D.
	23	0.34 ± 0.05	<D.L.	0.168 ± 0.020	N.A.	0.16 ± 0.11	N.D.	N.D.	N.D.
	30	0.54 ± 0.01	0.02 ± 0.00	0.247 ± 0.024	5.19 ± 0.53	<D.L.	N.D.	N.D.	N.D.
FSP2	3	10.20 ± 0.35	1.18 ± 0.01	0.048 ± 0.000	0.24 ± 0.02	11.30 ± 1.39	6.23 ± 0.00	5.34 × 10 <sup>5</sup>	1.29 × 10 <sup>5</sup>
	8	10.70 ± 0.30	0.93 ± 0.00	0.059 ± 0.000	0.39 ± 0.02	4.59 ± 0.80	0.48 ± 0.03	1.44 × 10 <sup>5</sup>	4.54 × 10 <sup>5</sup>
	13	11.31 ± 0.46	0.80 ± 0.01	0.019 ± 0.000	0.15 ± 0.01	5.01 ± 0.56	0.63 ± 0.04	1.72 × 10 <sup>5</sup>	4.13 × 10 <sup>5</sup>
	18	9.14 ± 1.12	0.58 ± 0.05	0.094 ± 0.015	0.87 ± 0.06	3.54 ± 0.47	0.55 ± 0.03	1.17 × 10 <sup>5</sup>	3.19 × 10 <sup>5</sup>
	23	7.29 ± 0.83	0.41 ± 0.02	N.D	N.D	1.95 ± 0.23	N.D.	N.D.	N.D.
	30	1.26 ± 0.19	0.05 ± 0.00	0.173 ± 0.025	2.54 ± 0.21	0.20 ± 0.11	N.D.	N.D.	N.D.
FSP3	38	0.52 ± 0.11	0.01 ± 0.00	0.182 ± 0.020	5.52 ± 0.45	0.44 ± 0.20	N.D.	N.D.	N.D.
	3	5.87 ± 0.37	0.50 ± 0.02	0.135 ± 0.015	0.93 ± 0.07	3.81 ± 0.94	0.33 ± 0.01	N.D.	N.D.
	8	6.02 ± 0.33	0.49 ± 0.02	0.050 ± 0.001	0.36 ± 0.01	1.57 ± 0.20	4.96 ± 0.25	N.D.	N.D.
	18	16.36 ± 0.16	0.95 ± 0.09	N.D	N.D.	3.42 ± 0.88	N.D.	N.D.	N.D.
	23	3.78 ± 0.04	0.18 ± 0.01	0.088 ± 0.010	1.08 ± 0.12	1.09 ± 0.17	N.D.	N.D.	N.D.
	30	1.28 ± 0.31	0.03 ± 0.00	0.159 ± 0.023	3.95 ± 0.24	<D.L.	N.D.	N.D.	N.D.
FSP4	3	6.93 ± 1.63	0.63 ± 0.18	0.341 ± 0.032	0.52 ± 0.04	8.87 ± 0.49	N.D.	N.D.	N.D.
	8	2.42 ± 0.12	0.18 ± 0.00	2.340 ± 0.030	0.91 ± 0.08	1.84 ± 0.28	9.23 ± 0.46	N.D.	N.D.
	13	0.98 ± 0.06	0.06 ± 0.00	4.674 ± 0.040	2.80 ± 0.12	1.07 ± 0.24	N.D.	N.D.	N.D.
	18	0.72 ± 0.02	0.05 ± 0.00	6.048 ± 0.053	1.66 ± 0.11	0.34 ± 0.21	N.D.	N.D.	N.D.
	23	0.90 ± 0.01	0.04 ± 0.00	13.671 ± 0.653	2.82 ± 0.13	1.02 ± 0.24	N.D.	N.D.	N.D.
	30	0.49 ± 0.16	0.02 ± 0.00	0.524 ± 0.002	3.17 ± 0.24	0.58 ± 0.00	N.D.	N.D.	N.D.
FSP0	surface	6.23 ± 0.08	0.08 ± 0.01	0.062 ± 0.002	2.80 ± 0.17	0.92 ± 0.12	0.07 ± 0.01	N.D.	N.D.
FSI18	surface	24.11 ± 1.09	1.46 ± 0.09	0.087 ± 0.004	0.84 ± 0.05	4.62 ± 0.31	N.D.	N.D.	N.D.

<sup>a</sup>Errors were reported as standard deviation of sample replicates: *n* = 2 for HS and <sup>239,240</sup>Pu measurement; *n* = 3 for organic carbon and total nitrogen measurement. N.D., not determined; <D.L. under detection limit; N.A., not available; errors were calculated on the basis of duplicates.

with diluted HF, yet this part should be minimal compared to the total sediment particulate hydroxamate content (see Results and Discussion). HF was then separated from the sample by centrifugation, and the pellet was thoroughly rinsed with 1 N HCl to eliminate any residual HF. The pellet was hydrolyzed in 1 mL of 3 M H<sub>2</sub>SO<sub>4</sub> at 100 °C for 4 h. Two aliquots (0.4 mL) of the hydrolyzed solution were transferred into two screw capped glass test tubes: one was used as the sample, and the other was used as a control to correct for interferences contributed by humic substances to the absorbance. For color development, the following reagents were successively added to both test tubes: (1) 1.4 mL of 2 M sodium acetate; (2) 0.4 mL of 1% (wt/vol) sulfanilamide in 30% (v/v) acetic acid; (3) 0.4 mL of 0.65% (wt/vol) iodine in 1% KI (wt/vol); (4) 0.4 mL of 1.5% (wt/vol) Na<sub>3</sub>AsO<sub>2</sub> solution to eliminate excess I<sub>2</sub>; (5) 0.4 mL of 0.05% α-naphthylamine (wt/vol) in nanopure water (18.2 MΩ) into the sample tube and 0.4 mL of nanopure water into the control tube. After allowing the tubes to stand for 18 h at room temperature for complete color development, the absorbance was measured at 543 nm. Absorbance of the control, to which α-naphthylamine was not added, was subtracted from that of the sample. This control correction was validated by adding Suwannee River fulvic acid in a concentration of 100 ppm organic carbon (Cat. #: 1S101F, IHSS) to 50 μM acetohydroxamic acid. The absorbance of fulvic acid-amended acetohydroxamic acid (with the addition of α-naphthylamine) was not significantly different from the sum

of absorbances of 50 μM acetohydroxamic acid without addition of fulvic acid and the control (acetohydroxamic acid amended with fulvic acid without the addition of α-naphthylamine). Acetohydroxamic acid was used for preparation of the calibrating standards (Cat. #: 159034, Sigma-Aldrich). This newly developed Csaky method, with two additional steps (the HF digestion and subtraction of the absorbance contributed by humic substances) compared to the traditional method, was first applied to determine the total sedimentary hydroxamate concentrations and has a detection limit of 1.5 μg of acetohydroxamic acid equivalent/g-sediment.

**Analysis of Pu-Carrying Colloidal Organic Macromolecules by ESI FTICR-MS.** Extraction and purification of sedimentary mobile Pu-carrying macromolecules is competed in 2014 and outlined in Figure S2. Sieved soil (<2 mm) was dispersed in 100g/20 L filtered artificial freshwater (<0.45 μm) with an ionic strength of 1.64 mM<sup>16,29</sup> and pH of ~5.0 (the average groundwater pH of the SRS F-Area<sup>36</sup>) for 3 days: (1) to simulate the release of mobile colloidal matter during groundwater exfiltration, surface runoff, and storm flow events; (2) to protect the structure and conformation of water-dispersible colloids without using any of the traditional harsh chemical treatments. A mobile colloidal fraction (1 kDa to 0.45 μm) was obtained from this slurry by filtration and cross-flow ultrafiltration. <sup>238</sup>Pu was spiked into this colloidal suspension (final <sup>238</sup>Pu concentration was 1.88 × 10<sup>-14</sup> M), allowed to reach equilibrium for 14 days,<sup>7</sup> and was subsequently



fractionated using isoelectric focusing gel electrophoresis.<sup>20,22</sup> The low pH section (pH 3.5–4.3), where one observed a significant <sup>238</sup>Pu peak (i.e., <sup>238</sup>Pu was enriched) (Figure S3), was cut from the gel, extracted with 1% SDS, and then diafiltered against nanopure water through a 1 kDa regenerated cellulose membrane in a stirred cell (Amicon Series 8200; Millipore Corporation, USA) to remove all the electrophoresis reagents. The retentate (>1 kDa) was freeze-dried, and this isolate is henceforth referred to as the “IEF extract”. IEF blank gels were treated the same way as sample gels throughout all extraction, diafiltration, and freeze-drying steps.

Both IEF extract and the blank were dissolved in nanopure water (18.2 MΩ) with 0.1% ammonium hydroxide, the latter of which was added as a volatile buffer.<sup>25,37</sup> The recovery of the organic matter, which was dissolved (the <0.2 μm fraction), was checked by a Shimadzu TOC 5000 Analyzer and reported as ~60%. The insoluble fraction was likely ascribed to more hydrophobic compounds. We assume the insoluble fraction is still partially dissolved, even not completely, as they originated from a water extraction. Immediately before conducting ESI FTICR-MS analyses, samples were diluted 1:1 (v/v) with LC-MS grade methanol and continuously fused into a Bruker Daltonics 12 T Apex Qe FTICR-MS with an Apollo II ESI ion source in the negative ionization mode, at the College of Science Major Instrumentation Cluster (COSMIC), Old Dominion University, Virginia. Duplicate samples were run to ensure reproducibility. In addition, desferrioxamine (DFO) (Cat #: D9533, Sigma-Aldrich, USA), a siderophore standard, was prepared in a similar manner as the sample and also analyzed by ESI FTICR-MS; its spectrum was compared with that of the IEF extract.

Mass spectra were externally calibrated with a polyethylene glycol standard and internally calibrated with fatty acids, dicarboxylic acids, and other naturally present CH<sub>2</sub> homologous series within the sample itself. All *m/z* lists, with an S/N ≥ 4, were exported for further data analysis. Furthermore, all *m/z* values shown in the procedure blank spectrum were excluded from the IEF extract mass list. A molecular formula calculator (Molecular Formula Calc version 1.0 NHMFL, 1998) generated empirical formula matches within 1.0 ppm using formula criteria of C<sub>(5–50)</sub>H<sub>(5–100)</sub>O<sub>(0–30)</sub>N<sub>(0–8)</sub>S<sub>(0–2)</sub>P<sub>(0–2)</sub>. Formulas were assigned according to previously described rules.<sup>26,28,38,39</sup> The double bond equivalent (DBE) was calculated as DBE = 1 + 0.5(2C–H + N + P). Peaks with (DBE)/C < 0.3 and H/C 1.0–3.0 were assigned as aliphatics.<sup>38</sup> Peaks with aromaticity indices (AI, calculated by (1 + C–O–S–0.5H)/(C–O–S–N–P)) greater than 0.5 and 0.67 were identified as aromatics and condensed aromatics, respectively.<sup>38,40</sup>

## RESULTS AND DISCUSSION

**Pu Concentrations and Isotopic Ratios in the Wetland Sediments.** Previous studies have reported Pu activity, isotopic composition, oxidation states, and association with colloids in groundwater downgradient of the disposal basins in the SRS F-Area.<sup>13,15</sup> Until recently, very little information was available about solid phase Pu, where the vast majority of Pu exists in this system.<sup>12</sup> Pu activity in FSP2 and FSP4 generally decreases with depth whereas a spike peak was observed in subsurface depths in both FSP1 (8 cm) and FSP3 (18 cm) cores (Table 1 and Figure S4), which is yet to be explained but likely related to the complex hydrological structures of the wetland.

Pu activity was not inversely correlated with the distance from the basins (Table 1 and Figure S1). A ranking of the samples based on distance from the seepage basin were: FSP3 < FSP2 < FSP4 < FSP1 (Figure S1). A ranking of the samples based on their surficial <sup>239,240</sup>Pu activity (<3 cm) were FSP2 > FSP4 > FSP1 > FSP3 (Table 1). Previous research has shown that the impact of the plume on the wetlands is extremely heterogeneous, resulting in part from differences in preferential groundwater flow paths.<sup>41</sup> However, comparing the average value of all measured <sup>239,240</sup>Pu activities of wetland sediment samples from this study (2.8 Bq/kg; assuming that all below detection limit values were equal to 0 Bq/kg) to that of the upland sediments measured in Kurosaki et al.<sup>12</sup> (1.1 Bq/kg), the wetland sediment <sup>239,240</sup>Pu concentrations were ~2.5 greater than the upland sediments, in which the organic carbon concentrations were very low (<0.01 wt %). Furthermore, the upland sediments were closer to the source term (the seepage basin) and as such would be expected to have greater Pu concentrations than the more distant wetland sediments. Complicating this simplified description of Pu distribution in F-Area is the observation that <sup>244</sup>Cm released from the seepage basin was much more mobile than <sup>239,240</sup>Pu and was concentrated downgradient of the seepage basin, resulting in an elevated <sup>240</sup>Pu concentration derived from <sup>244</sup>Cm decay, in both the groundwater<sup>13,42</sup> and sediments.<sup>12</sup> The isotopic ratios, <sup>240</sup>Pu/<sup>239</sup>Pu of the wetland sediments (0.33–9.23, Table 1), were appreciably higher than those reported in sediments collected upgradient to the wetlands (0.23–0.39),<sup>12</sup> which could be ascribed to (1) more <sup>240</sup>Pu derived from <sup>244</sup>Cm decay (half-life = 18.1 years) during the six years elapsing between the measurement by Kurosaki et al.<sup>12</sup> (2006) and those reported here (2012); (2) samples from the two studies originated from different depths (top 0.38 m in this study vs 18–22 m in Kurosaki et al.<sup>12</sup>). Nevertheless, <sup>240</sup>Pu/<sup>239</sup>Pu isotopic ratios in nearby groundwater samples (ratios = 3–8) fall at the high end of the range of those determined in these wetland sediments,<sup>13,42</sup> suggesting a likelihood of similar <sup>240</sup>Pu (and/or <sup>239</sup>Pu) origins (from the original source term, i.e., seepage basin, and *in situ* <sup>240</sup>Pu ingrowth) and environmental controls (pH, redox, and association with colloids) of the two Pu isotopes.<sup>13,15</sup>

Total <sup>239,240</sup>Pu activity in the surficial sediment in FSP0, as a “background” site least affected by contaminant groundwater plume in the wetland region, was 4–12 times lower than the other sediments along the seepage basin-groundwater-wetland pathway (FSP1-4 and FSI18). The global fallout has an average <sup>240</sup>Pu/<sup>239</sup>Pu ratio of 0.18. However, the <sup>240</sup>Pu/<sup>239</sup>Pu isotopic ratio (0.07 ± 0.01) at FSP0 was close to that expected from SRS reactor operations (~0.062), suggesting local atmospheric deposition originating from the reactor operation is likely the primary source of Pu, and constituted the sedimentary Pu baseline in F-Area.

In addition to the apparent concentrating effect of wetland in <sup>239,240</sup>Pu activity, the empirical <sup>239</sup>Pu (or <sup>240</sup>Pu) concentration solid/water ratios were calculated (eq 1):

$$\text{Pu concentration solid/water ratios} = \frac{[C]_{\text{sediment}}}{[C]_{\text{groundwater}}} \quad (1)$$

where  $[C]_{\text{sediment}}$  and  $[C]_{\text{groundwater}}$  are the <sup>240</sup>Pu (or <sup>239</sup>Pu) concentrations in the sediment (atoms/kg) and the groundwater (atoms/L), respectively. The  $[C]_{\text{sediment}}$  data were taken from Table 1, whereas the  $[C]_{\text{groundwater}}$  data were adapted from

a nearby well (Well 4) reported by Buesseler et al.<sup>13</sup> and Dai et al.,<sup>15</sup> which is the approximate aqueous Pu concentrations based on the best available literature values, with similar <sup>240</sup>Pu/<sup>239</sup>Pu ratios (see above). These <sup>239</sup>Pu (or <sup>240</sup>Pu) concentration solid/water ratios were comparable to laboratory log  $K_d$  values (5–6) using humic acids extracted from the F-Area wetland sediments,<sup>7</sup> but a few orders of magnitude higher than those in Kurosaki et al.,<sup>12</sup> in which upgradient sediment with low organic carbon concentrations and the same mineral formation was used. These Pu concentration solid/water ratios calculated in this manner might be compromised in-so-far that the aqueous and solid phases are not necessarily in close contact (and thus not at equilibrium either), and the heterogeneous characteristic of the wetland system should also be taken as a cautionary note. Given these important caveats, it appears that NOM may be an important control of Pu biogeochemical behavior in the wetland sediment and will be explored in the sections below.

**Supporting Evidence of Hydroxamate Siderophores (HS) as One of the N-Containing Compounds Responsible for Pu Immobilization.** Previous studies on soil siderophores were mostly focused on soil solution<sup>24</sup> or soil extractants by water or methanol.<sup>23,43,44</sup> This study, for the first time, explored the occurrence of HS moieties that are incorporated into the sediment particulate organic matter and released from the macromolecules upon the HF digestion and H<sub>2</sub>SO<sub>4</sub> hydrolysis. Understanding the binding environment of Pu in the solid phase, as opposed to the aqueous phase, is especially important because the vast majority of Pu in the environment is associated with solids. In fact, HS concentrations in the water or methanol extract (aqueous/sediment 1:1) were not detectable by the Csaky assay (data not shown). The dissolved (“water extracted”) and adsorbed (“methanol extracted”) siderophores were previously reported in the range of  $2.6 \times 10^{-9}$  to  $4.9 \times 10^{-7}$  and  $5.8 \times 10^{-9}$  to  $4.0 \times 10^{-7}$  g-C/g-OC, respectively,<sup>23</sup> and were a few orders of magnitude lower than the total HS determined in the sediment particulate phase by our study (Table 1,  $1.9 \times 10^{-5}$  to  $1.4 \times 10^{-2}$  g-C/g-OC in dry soil). HS concentrations not only moderately correlate with sedimentary organic carbon contents (Figure S5a), which is consistent with the findings by Powell et al.,<sup>44</sup> but also with total nitrogen contents (Figure S5b).

Total <sup>239,240</sup>Pu activity was positively and moderately correlated with sedimentary organic carbon content (Figure S5c,  $R = 0.561$ ,  $p \leq 0.01$ ,  $df = 21$ ). It is noteworthy that total <sup>239,240</sup>Pu activity was more strongly related to total nitrogen contents ( $R = 0.731$ ,  $p \leq 0.001$ ,  $df = 21$ ) and HS concentrations ( $R = 0.975$ ,  $p < 0.001$ ,  $df = 19$ ) (Figure 1). Even if the data point with the highest HS concentration and <sup>239,240</sup>Pu activity, which might seem to drive the linear regression, is removed, the rest of the data points still confirm a significant correlation ( $R = 0.9239$ ,  $p < 0.001$ ,  $df = 18$ ). This strongly suggests that N-containing organic compounds out of the bulk sedimentary organic matter pool are involved in (or related to) Pu immobilization, and HS could be one of the main Pu complexing ligands.

At low Fe/NOM ratios (e.g., <12 mg Fe/g-NOM), it is well-known that Fe/NOM complexes are the dominant iron-bearing species in soils or sediments and suppress the hydrolysis of Fe.<sup>45</sup> At higher Fe/NOM ratios (e.g., >~20 mg Fe/g-NOM<sup>45</sup>), mixtures of Fe/NOM complexes and polymeric Fe(III) (hydr)oxide phases are coexistent,<sup>45–47</sup> with the latter being

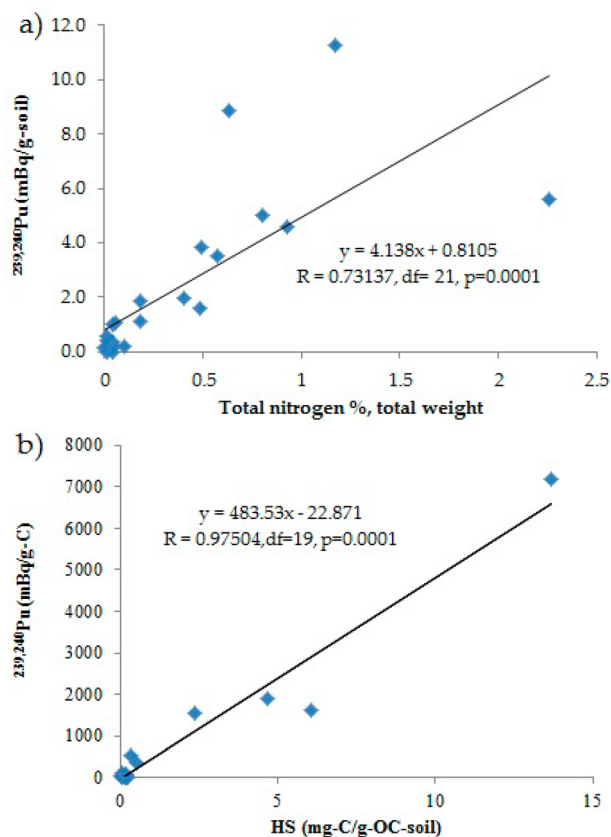


**Figure 1.** Correlation relationships between total <sup>239,240</sup>Pu activity and (1) total nitrogen contents; (2) hydroxamate siderophores (HS) concentrations (in acetohydroxamic acid equivalents and normalized to organic carbon (mg-C/g-OC-soil)) in wetland sediment samples collected from F-Area of the SRS.

still associated with NOM through electrostatic interaction, hydrogen bonding, ligand exchange-surface complexation, hydrophobic interaction, etc.<sup>48</sup> Being similar to Fe(III) in ionic potential, i.e., ratios of charge to ionic size and hydrolysis properties (tendency to form oxyhydroxides), other “hard-acid” metal ions such as Pu(IV) and Th(IV) can form strong complexes with ligands containing “hard” donor atoms (e.g., O) and thus also exhibit strong affinity toward siderophores.<sup>49,50</sup> The conditional stability constant for Fe(III) and trihydroxamate desferrioxamine (DFO) siderophore complex at neutral pH is 30.5 ( $H^+ + DFOB^{3-} + Fe(III) \leftrightarrow Fe(III)HDFOB^+$ )<sup>23</sup> and that for Pu(IV) and DFO is about 30.8 ( $H^+ + DFOB^{3-} + Pu(IV) \leftrightarrow Pu(IV)HDFOB^{2+}$ ).<sup>51</sup> The similarity of these two constants is supportive of the similarity between Fe(III) and Pu(IV) complexation chemistry. Furthermore, these values are greater than commercially available chelates (citrate, EDTA, and Tiron), providing additional support for the argument that these hydroxamate siderophores likely influence Pu complexation in natural systems.

**Direct Identification of HS Moieties in a Pu Vector Using ESI FTICR-MS.** In a previous laboratory study with SRS wetland sediment, potentially mobile Pu was found to be almost exclusively (>95%) associated with colloidal organic matter (1 kDa to 0.45  $\mu$ m fraction).<sup>7</sup> In this study, the low pH fraction (pH 3.5–4.3) obtained from IEF separation contained ~50% of the Pu that was spiked into the water extractable colloid suspension (1 kDa to 0.45  $\mu$ m fraction of the soil-water

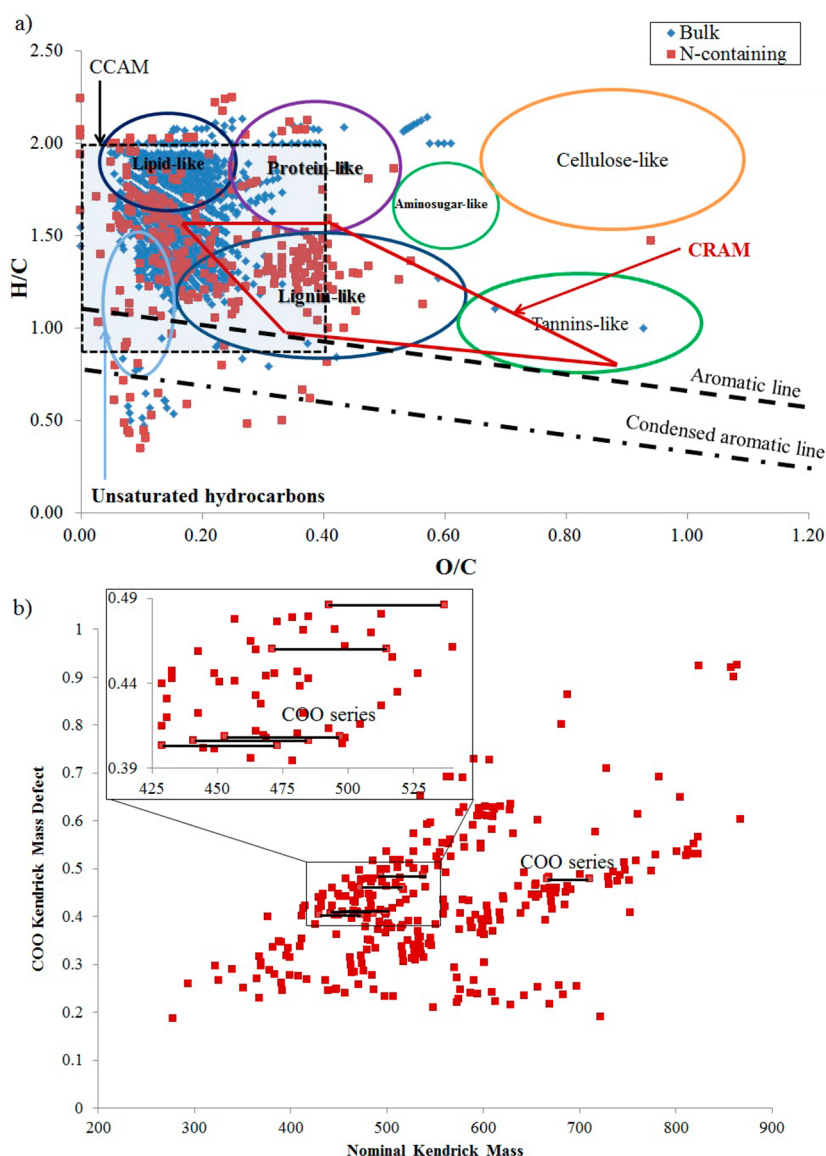


**Figure 2.** (a) van Krevelen diagram showing all 1259 formulas and the N-containing formulas of the IEF extract; (b) Kendrick mass defect (KMD) plot of peaks on the trend line analyzed by COO KMD analysis (carboxylic-rich alicyclic molecules (CRAM) = double bond equivalent (DBE)/C = 0.30–0.68, DBE/H = 0.20–0.95, DBE/O = 0.77–1.75; carboxyl-containing aliphatic molecules (CCAM) = O/C 0–0.40, H/C 0.85–2.00).

**Table 2. Molecular Information for the Bulk IEF Extract (the Pu Binding Molecules Obtained through Isoelectric Focusing Separation) and Its N-Containing Compounds, as Revealed by ESI FTICR-MS<sup>a</sup>**

molecular class	bulk			N-containing		
	no. of peaks	% peak intensity	average MW	no. of peaks	% peak intensity	average MW
all identified formula	1259	100	485	291	100	526
aliphatics (DBE/C < 0.3; H/C 1.0–3.0)	813	67.81	474	223	74.43	515
aromatics (AI > 0.5)	42	3.36	575	26	7.54	582
condensed aromatics (AI ≥ 0.67)	31	2.64	579	19	5.74	595
black carbon-like CARS (DBE/C > 0.7)	30	2.57	580	18	5.46	595
Kim et al. <sup>68</sup>	4	0.37	632	3	1.01	654
CRAM	139	9.30	514	80	21.95	542
CCAM	1143	87.57	487	233	85.36	516

<sup>a</sup>AI, aromaticity index (AI = (1 + C–O–C–0.5H)/(C–O–S–N–P)); CARS, condensed aromatic ring structure; MW, molecular weight (normalized by intensity); Kim et al.<sup>68</sup> definition of black carbon-like molecules = O/C 0.3–0.6, H/C 0.5–0.8; carboxylic-rich alicyclic molecules (CRAM) = double bond equivalent (DBE)/C = 0.30–0.68, DBE/H = 0.20–0.95, DBE/O = 0.77–1.75; carboxyl-containing aliphatic molecules (CCAM) = O/C 0–0.40, H/C 0.85–2.00).



slurry) (Figures S2 and S3). The remaining Pu activity was distributed in appreciably lower concentrations throughout the remaining fractions of the IEF gel (pH 4.3–10). Even though ESI FTICR-MS is semiquantitative due to its selective ionization efficiencies toward different classes of compounds, it still gives the relative abundance of various heteroatom compounds of the Pu carrying macromolecules, by providing the percentages sorted by peak number and peak intensity, respectively. It is shown that the IEF extract consisted primarily of CHO-only formulas (61% and 47% by peak number and peak intensity, respectively, the same below) and lesser amounts of CHON (17% and 22%) and CHOS (14% and 23%) (Figure S6).

A total of 1259 formulas were identified and assigned for the IEF extract, which is a subfraction of the bulk mobile colloidal fraction of sediment aggregate and enriches most of the spiked Pu. Of all these formulas, 291 contain nitrogen. A van Krevelen diagram of all formulas is displayed in Figure 2a, and associated molecular information is presented in Table 2. There are fewer peaks detected in this “IEF extract” than in a typical terrestrial NOM sample by the negative ionization mode of FTICRMS,<sup>52,53</sup> which could be ascribed to the partial dissolution of the sample (~60% recovery rate) and low ionization efficiency and/or most likely to the fact that the “IEF extract” is relatively a more homogeneous, purified segment of the bulk NOM. Regardless, these Pu binding molecules, which were isolated from the sediment through water extraction and isoelectric focusing electrophoresis separation, are responsible for complexing the majority of potentially mobile Pu and are mainly aliphatic (65% in peak number and 68% in peak intensity, respectively), with some minor aromatics (defined as AI > 0.5). N-containing compounds that likely include the strongest Pu-binding ligands were also dominated by aliphatics (77% in peak number and 74% in peak intensity, respectively) with slightly elevated aromatics, condensed aromatics, and black carbon contents compared to the bulk polymers. Formulas assignable as carboxylic-rich alicyclic molecules (CRAM), which occupy a very certain yet restricted area of compositional space (DBE/C 0.30–0.68, DBE/H 0.20–0.95, DBE/O 0.77–1.75), were more pronounced in the N-containing compound pool, compared to the bulk IEF extract (27% vs 11% in peak number and 22% vs 9% in peak intensity).<sup>54</sup> However, formulas assignable as CRAM can also be assigned as lignin, as evidenced by the overlapping in the van Krevelen diagram between CRAM and lignin (Figure 2a). The presence of N in CRAM has not previously been reported,<sup>54</sup> whereas N in the lignin derivatives has been mainly attributed to peptide or N-acetyl (CO–NH–CHR) and anilide (CO–NH–C<sub>aromatic</sub>) structures and other minor functional groups.<sup>55</sup> Moreover, N bonded to lignin derivatives are known to be less bioavailable<sup>55</sup> and thus more recalcitrant. Recently, Hartman et al.<sup>56</sup> referred to molecules covering the van Krevelen diagram with H/C 0.85–2.00 and O/C 0–0.40 as carboxyl-containing aliphatic (number of COO–R functionality ≥ 1) and/or alicyclic molecules (CCAM) (Figure 2a). These molecules, covering a region that overlaps those for all the lipid-like, partially protein-like, unsaturated hydrocarbons, lignin-like, and traditionally defined CRAM, and with H/C ratios being centered at 1.4, are suggested to be alicyclic and/or olefinic, rather than saturated/linear or branched aliphatic molecules.<sup>56</sup> CCAM-type moieties account for the majority of both the bulk Pu carrying macromolecules (87.57% of the “IEF extract”) and the N-containing compounds (85.36%) (Table 2).

It is noticeable that three significant peaks in the ESI FTICR-MS spectrum of DFO were identified in that of the “IEF extract” (Table S2), suggesting that these Pu carrying polymeric macromolecules contain functionalities of this HS standard. Likely, there could have been more types of HS in the particulate and colloidal fractions of the sediment aggregates. Our analysis was limited by the availability of standard reference materials, as only DFO was analyzed with ESI FTICR-MS and its spectrum compared with that of the “IEF extract”. It is expected that, if more HS reference materials were presently available, more hydroxamate compounds would have been identified. However, it is unlikely that HS moieties were present as individual low molecular weight compounds as previously detected in the dissolved and adsorbed phases,<sup>23,24,43,44</sup> because (1) the majority of the HS functionality in the sediment could only be substantially released after the acid digestion (HF) and hydrolysis (H<sub>2</sub>SO<sub>4</sub> with heat) steps and then quantitatively determined by the spectrophotometric method; (2) the “IEF extract” originated from sediment/water slurry and was obtained as a colloidal fraction through the processes of filtration and ultrafiltration (1 kDa to 0.45 μm); (3) the colloidal organic fraction was determined to have molecular weights of (3.6 ± 0.4) kDa and (103.8 ± 2.5) kDa with HPLC-size exclusion chromatography.<sup>16</sup> There is no disagreement that the HS moieties were actually detected in the molecular weight range of 200–1000 Da by ESI FTICR-MS, as NOM has been demonstrated to consist of clusters of diverse, low molecular mass components forming dynamic high molecular macromolecules and even micellar structures through hydrophobic interaction and hydrogen bonds, in aqueous environments.<sup>37,57</sup>

How the low molecular weight HS becomes part of particulate organic matter and colloidal organic matter fractions of the sediment is not entirely clear, as the expected tendency of HS release would be to solubilize Fe from mineral phases to provide bioavailable Fe(III) for microbes. In fact, nitrogen contributed by HS to the total N of the sediment amounts to a very minor fraction (0.02–0.55% of total sedimentary N, Table 1); thus, it is not surprising that its presence in the high molecular weight fraction of the sediment or soil aggregates was so far not recognized and scarcely studied, except by Chuang et al.<sup>50</sup> Our hypothetical scheme of HS incorporation into particulate organic matter and colloidal organic matter is described as follows. On one hand, siderophores are decomposed, destroyed, or recycled upon enzymatic reduction and degradative processes.<sup>58,59</sup> On the other hand, HS functional groups are likely incorporated into high molecular macromolecules through repolymerization or cyclization reactions aided by enzymatically regulated superoxide and hydroxyl radical formation.<sup>60</sup> This type of process has been suggested for the “imbedding” or cross-linking of lignin in the hemicellulose matrix<sup>61</sup> and could also be one of the likely mechanisms that HS moieties survive harsh conditions in particulate or colloidal phases of soil aggregates in the environment. Kendrick mass defect (KMD) analysis of the N-containing compounds, based on COO group formulation<sup>26</sup> (eq 2), yields a series of points horizontally aligned on a KMD plot indicating they belong to a homologous series, i.e., formulas with the same KMD value differing only by the number of carboxyl (COO) groups (Figure 2b). The presence of significant amounts of series differing by COO groups supports that (1) some of the N-containing compounds are carboxyl-substituted, a structure required by hydroxamate, and



(2) formation of compounds present in the aliphatic region through the radical polymerization processes followed by loss of carboxyl groups, proposed by Waggoner et al.,<sup>60</sup> might likely occur to these N-containing moieties.

$$\text{Kendrick Mass} = \text{exact } m/z \text{ of peak} \\ \times (44.000000000/43.989829244)$$

$$\text{Kendrick Mass Defect (KMD)}$$

$$= \text{observed nominal mass} - \text{Kendrick mass} \quad (2)$$

Alternatively, the surviving HS moieties might be preserved, “knitted”, and stabilized into particulate or colloidal organic macromolecular meshes through the actions of biosurfactants,<sup>62,63</sup> hydrophobic interactions (van der Waals,  $\pi$ - $\pi$ , CH- $\pi$ , etc.), or hydrogen bonding with other NOM.<sup>64–66</sup> It is possible that complexation with polyvalent cations (e.g., Fe<sup>3+</sup>, Pu(IV)) in a six coordinate pseudo-octahedral geometry through O-ligands also provides additional protection for these N-containing moieties to survive for longer periods of time in the sediment.<sup>67</sup> A piece of supporting evidence is from the acidic hydrolysis of both the sediment and monohydroxamate standard acetohydroxamic acid (HO-NH-COOH). After the acidic hydrolysis procedure, the responses of acetohydroxamic acid standards of various concentrations (5–1000  $\mu$ M) to the Csaky test reagents were not significantly different from those without acidic hydrolysis (Figure S7). The linearity of the responses of different amounts of sediment (0.5, 1, and 2 g) to the Csaky test reagents, after subsection to the acidic hydrolysis, is also good ( $R^2 = 0.95$ ).

By combining direct evidence (ESI FTICR-MS identification of the specific Pu carrying macromolecules after their separation from the bulk particulate organic matter) and indirect evidence (the correlation relationship between total sedimentary <sup>239,240</sup>Pu and HS concentrations), this study provided novel support for the idea that HS moieties, present as a very minor component in the sedimentary particulate organic matter or colloidal organic matter, may play a pivotal role in Pu immobilization/remobilization in the far-field wetland sediments of the SRS F-Area. As HS only contributes a very small portion to the total nitrogen in the “IEF extract”, it seems likely that other N-containing compounds (primarily as aliphatics and CRAM) also contribute to the positive correlation between total sedimentary <sup>239,240</sup>Pu concentration and total nitrogen contents (Figure 1). Further studies of these N-containing compounds are warranted. It is also recommended that positive ionization mode of ESI FTICR-MS be applied to provide complementary information on these compounds.

If one takes the HS contents (Table 1) and assumes that all Pu is bound in a mononuclear and octahedral configuration to the HS moieties in the sediments, similar to Fe/NOM interactions in the natural environment (i.e., Pu/HO-NH-COOH in a ratio of 1:3),<sup>45–47</sup> it would yield a total binding intensity of  $3.0 \times 10^{-8}$  to  $7.9 \times 10^{-7}$  mol/kg-sediment of <sup>239,240</sup>Pu (see Table S3 for detailed deduction). This is 5 orders of magnitude higher than the actual sedimentary Pu concentrations ( $8.9 \times 10^{-13}$  to  $6.2 \times 10^{-12}$  mol/kg-sediment). Even only taking the relative abundance (peak intensity) of the three formulas (Table S2) characteristic of DFO compounds over that of the total N-containing formulas (N-DFO/total nitrogen 1:200), the HS ligands are still in surplus. With the

high conditional stability constant of Pu/HS complex ( $K_a = \sim 30$ ), it is likely that HS is one of the strongest binding agents in the sediment for Pu.

Overall, this Pu carrier is somewhat similar (but more detailed) to what has been identified by ATR-FTIR, <sup>13</sup>C DPMAS NMR, 1D <sup>1</sup>H HRMAS NMR, 2D <sup>1</sup>H-<sup>1</sup>H COSY, and <sup>1</sup>H-<sup>13</sup>C HSQC NMR techniques, in the surface soil of Rocky Flats Environmental Technology Site (RFETS),<sup>22</sup> in that both are composed of aliphatic backbones with HS moieties and other N-containing compounds. However, these two Pu carriers originated from sources of different biopolymer precursors, due to profoundly different site vegetation (perennial grassland in RFETS vs herbaceous, woody, and swamp wetland in SRS) and different biogeochemical environments (arid, windy, intense solar radiation, large daily and seasonal temperature ranges in the RFETS vs warm, humid climate and relatively mild daily and seasonal temperature ranges in the SRS). These factors are expected to result in differences in the fine architectures of the Pu carrying vectors from these two sites. Pu (more specifically <sup>240</sup>Pu), originating from <sup>244</sup>Cm decay in the downgradient wetland area of the SRS F-Area, was reported to be initially in a relatively mobile form.<sup>13</sup> Yet Pu has been shown to be likely scavenged by the N-containing compounds, such as hydroxamate siderophores, in the wetland sediment organic matter, resulting in elevated sedimentary <sup>239,240</sup>Pu activity and <sup>239</sup>Pu (or <sup>240</sup>Pu) concentration solid/water ratios, compared to those in the upland nonwetland sediment. This study provides additional information supporting the conclusion that hydroxamate siderophores are important moieties within NOM for complexing Pu. For the first time, the role of hydroxamate siderophores in soils on Pu partitioning has been studied. This conclusion is based on studying Pu at environmentally relevant concentrations, in the femtomolar range, so as not to introduce experimental artifacts caused by flooding NOM binding sites with elevated Pu concentrations to ease analytical detection. However, unfortunately, direct spectroscopic evidence linking hydroxamate siderophores and Pu at these concentrations remains elusive and requires indirect approaches. These novel results showing the presence of hydroxamates in the particulate soil fraction (rather than in solution) and their relationship to the presence of Pu have profound implications for the on-site radiological risk evaluation. This also underscores the involvement of specific NOM compounds in immobilizing and remobilizing radionuclides in wetland sediments, which could behave as either a sink or source of contaminants to the neighboring environmental compartments.

## ■ ASSOCIATED CONTENT

### ● Supporting Information

The Supporting Information is available free of charge on the ACS Publications website at DOI: 10.1021/acs.est.5b02310.

Details of Pu determination by alpha spectrometry and ICP-MS (PDF)

## ■ AUTHOR INFORMATION

### Corresponding Author

\*Phone: +1-409-740-4530; fax: 1-409-740-4787; e-mail: xuc@tamug.edu.

### Author Contributions

The authors declare no competing financial interest.

## 699 Notes

700 The authors declare no competing financial interest.

## 701 ■ ACKNOWLEDGMENTS

702 This work was funded by DOE SBR Grant #DE-ER64567-  
703 1031562-0014364. M.A. was partially funded by Welch Grant  
704 BD0046. We thank Susan Hatcher and Jared Callan at the  
705 COSMIC (College of Science Major Instrumentation Cluster)  
706 facility at Old Dominion University for their assistance with the  
707 ESI FTICR-MS analyses. We are very thankful for the  
708 constructive comments from four anonymous reviewers that  
709 improved this manuscript.

## 710 ■ REFERENCES

711 (1) Zeng, T.; Ziegelgruber, K. L.; Chin, Y. P.; Arnold, W. A. Pesticide  
712 Processing Potential in Prairie Pothole Porewaters. *Environ. Sci.*  
713 *Technol.* **2011**, *45* (16), 6814–6822.  
714 (2) Zeng, T.; Ziegelgruber, K. L.; Chin, Y. P.; Arnold, W. A. Pesticide  
715 Processing Potential in Prairie Pothole Porewaters. *Environ. Sci.*  
716 *Technol.* **2012**, *46* (20), 11482–11482.  
717 (3) Zeng, T.; Arnold, W. A. Pesticide Photolysis in Prairie Potholes:  
718 Probing Photosensitized Processes. *Environ. Sci. Technol.* **2013**, *47*  
719 (13), 6735–6745.  
720 (4) Gambrell, R. P. Trace and Toxic Metals in Wetlands - a Review.  
721 *Journal of Environmental Quality* **1994**, *23* (5), 883–891.  
722 (5) Quinto, F.; Hrncsek, E.; Krachler, M.; Shotyk, W.; Steier, P.;  
723 Winkler, S. R. Determination of <sup>239</sup>Pu, <sup>240</sup>Pu, <sup>241</sup>Pu and <sup>242</sup>Pu at  
724 femtogram and attogram levels - evidence for the migration of fallout  
725 plutonium in an ombrotrophic peat bog profile. *Environmental Science:*  
726 *Processes & Impacts* **2013**, *15* (4), 839–847.  
727 (6) Wang, Y.; Fruttschi, M.; Suvorova, E.; Phrommavanh, V.;  
728 Descostes, M.; Osman, A. A. A.; Geipel, G.; Bernier-Latmani, R.  
729 Mobile uranium(IV)-bearing colloids in a mining-impacted wetland.  
730 *Nat. Commun.* **2013**, *4*, 2942.  
731 (7) Xu, C.; Athon, M.; Ho, Y.-F.; Chang, H.-S.; Zhang, S.; Kaplan, D.  
732 I.; Schwehr, K. A.; DiDonato, N.; Hatcher, P. G.; Santschi, P. H.  
733 Plutonium Immobilization and Remobilization by Soil Mineral and  
734 Organic Matter in the Far-Field of the Savannah River Site, U.S.  
735 *Environ. Sci. Technol.* **2014**, *48* (6), 3186–3195.  
736 (8) Powell, B. A.; Duff, M. C.; Kaplan, D. I.; Fjeld, R. A.; Newville,  
737 M.; Hunter, D. B.; Bertsch, P. M.; Coates, J. T.; Eng, P.; Rivers, M. L.;  
738 Sutton, S. R.; Triay, I. R.; Vaniman, D. T. Plutonium oxidation and  
739 subsequent reduction by Mn(IV) minerals in Yucca Mountain tuff.  
740 *Environ. Sci. Technol.* **2006**, *40* (11), 3508–3514.  
741 (9) Powell, B. A.; Fjeld, R. A.; Kaplan, D. I.; Coates, J. T.; Serkiz, S.  
742 M. Pu(V)O<sub>2</sub>(+) adsorption and reduction by synthetic magnetite  
743 (Fe<sub>3</sub>O<sub>4</sub>). *Environ. Sci. Technol.* **2004**, *38* (22), 6016–6024.  
744 (10) Powell, B. A.; Fjeld, R. A.; Kaplan, D. I.; Coates, J. T.; Serkiz, S.  
745 M. Pu(V)O<sub>2</sub>(+) adsorption and reduction by synthetic hematite and  
746 goethite. *Environ. Sci. Technol.* **2005**, *39* (7), 2107–2114.  
747 (11) Powell, B. A.; Kaplan, D. I.; Serkiz, S. M.; Coates, J. T.; Fjeld, R.  
748 A. Pu(V) transport through Savannah River Site soils – an evaluation  
749 of a conceptual model of surface-mediated reduction to Pu(IV). *J.*  
750 *Environ. Radioact.* **2014**, *131*, 47.  
751 (12) Kurosaki, H.; Kaplan, D. I.; Clark, S. B. Impact of  
752 Environmental Curium on Plutonium Migration and Isotopic  
753 Signatures. *Environ. Sci. Technol.* **2014**, *48* (23), 13985–13991.  
754 (13) Buesseler, K. O.; Kaplan, D. I.; Dai, M.; Pike, S. Source-  
755 dependent and source-independent controls on plutonium oxidation  
756 state and colloid associations in groundwater. *Environ. Sci. Technol.*  
757 **2009**, *43* (5), 1322–1328.  
758 (14) Arnett, M. W. *Savannah River Site Environmental Data for 1992*;  
759 Westinghouse Savannah River Company: Aiken, South Carolina, 1993.  
760 (15) Dai, M.; Kelley, J. M.; Buesseler, K. O. Sources and migration of  
761 plutonium in groundwater at the Savannah River Site. *Environ. Sci.*  
762 *Technol.* **2002**, *36* (17), 3690–3699.

(16) Xu, C.; Zhang, S.; Ho, Y.-F.; Miller, E. J.; Roberts, K. A.; Li, H.-  
763 P.; Schwehr, K. A.; Otsuka, S.; Kaplan, D. I.; Brinkmeyer, R.; Yeager,  
764 C. M.; Santschi, P. H. Is soil natural organic matter a sink or source for  
765 mobile radioiodine (<sup>129</sup>I) at the Savannah River Site? *Geochim.*  
766 *Cosmochim. Acta* **2011**, *75* (19), 5716–5735.  
767 (17) Schwehr, K. A.; Santschi, P. H.; Kaplan, D. I.; Yeager, C. M.;  
768 Brinkmeyer, R. Organo-Iodine Formation in Soils and Aquifer  
769 Sediments at Ambient Concentrations. *Environ. Sci. Technol.* **2009**,  
770 *43* (19), 7258–7264.  
771 (18) Kaplan, D. I.; Roberts, K. A.; Schwehr, K. A.; Lilley, M. S.;  
772 Brinkmeyer, R.; Denham, M. E.; Diprete, D.; Li, H. P.; Powell, B. A.;  
773 Xu, C.; Yeager, C. M.; Zhang, S. J.; Santschi, P. H. Evaluation of a  
774 radioiodine plume increasing in concentration at the Savannah River  
775 Site. *Environ. Sci. Technol.* **2011**, *45* (2), 489–495.  
776 (19) Emerson, H. P.; Xu, C.; Ho, Y.-F.; Zhang, S.; Schwehr, K. A.;  
777 Lilley, M. S.; Kaplan, D. I.; Santschi, P. H.; Powell, B. A. Geochemical  
778 controls of iodine uptake and transport in Savannah River Site  
779 subsurface sediments. *Appl. Geochem.* **2014**, *45*, 105–113.  
780 (20) Santschi, P. H.; Roberts, K. A.; Guo, L. D. Organic nature of  
781 colloidal actinides transported in surface water environments. *Environ.*  
782 *Sci. Technol.* **2002**, *36* (17), 3711–3719.  
783 (21) Roberts, K. A.; Santschi, P. H.; Leppard, G. G.; West, M. M.  
784 Characterization of organic-rich Pu-239, Pu-240-containing colloids  
785 from surface and ground waters from a contaminated site in Colorado,  
786 USA. *Geochim. Cosmochim. Acta* **2004**, *68* (11), A507.  
787 (22) Xu, C.; Santschi, P. H.; Zhong, J. Y.; Hatcher, P. G.; Francis, A.  
788 J.; Dodge, C. J.; Roberts, K. A.; Hung, C. C.; Honeyman, B. D.  
789 Colloidal cutin-like substances cross-linked to siderophore decom-  
790 position products mobilizing plutonium from contaminated soils.  
791 *Environ. Sci. Technol.* **2008**, *42* (22), 8211–8217.  
792 (23) Ahmed, E.; Holmström, S. J. M. The effect of soil horizon and  
793 mineral type on the distribution of siderophores in soil. *Geochim.*  
794 *Cosmochim. Acta* **2014**, *131* (0), 184–195.  
795 (24) Essén, S.; Bylund, D.; Holmström, S. M.; Moberg, M.;  
796 Lundström, U. Quantification of Hydroxamate Siderophores in Soil  
797 Solutions of Podzolic Soil Profiles in Sweden. *BioMetals* **2006**, *19* (3),  
798 269–282.  
799 (25) Kujawinski, E. B. Electrospray Ionization Fourier Transform Ion  
800 Cyclotron Resonance Mass Spectrometry (ESI FT-ICR MS):  
801 Characterization of Complex Environmental Mixtures. *Environ.*  
802 *Forensics* **2002**, *3* (3–4), 207–216.  
803 (26) Sleighter, R. L.; Hatcher, P. G. The application of electrospray  
804 ionization coupled to ultrahigh resolution mass spectrometry for the  
805 molecular characterization of natural organic matter. *J. Mass Spectrom.*  
806 **2007**, *42* (5), 559–574.  
807 (27) Hixon, A. E.; Powell, B. A. Observed Changes in the Mechanism  
808 and Rates of Pu(V) Reduction on Hematite As a Function of Total  
809 Plutonium Concentration. *Environ. Sci. Technol.* **2014**, *48* (16), 9255–  
810 9262.  
811 (28) Xu, C.; Chen, H.; Sugiyama, Y.; Zhang, S.; Li, H.-P.; Ho, Y.-F.;  
812 Chuang, C.-y.; Schwehr, K. A.; Kaplan, D. I.; Yeager, C.; Roberts, K.  
813 A.; Hatcher, P. G.; Santschi, P. H. Novel molecular-level evidence of  
814 iodine binding to natural organic matter from Fourier transform ion  
815 cyclotron resonance mass spectrometry. *Sci. Total Environ.* **2013**, *449*  
816 (0), 244–252.  
817 (29) Xu, C.; Miller, E. J.; Zhang, S. J.; Li, H. P.; Ho, Y. F.; Schwehr,  
818 K. A.; Kaplan, D. I.; Otsuka, S.; Roberts, K. A.; Brinkmeyer, R.;  
819 Yeager, C. M.; Santschi, P. H. Sequestration and Remobilization of  
820 Radioiodine (I-129) by Soil Organic Matter and Possible Con-  
821 sequences of the Remedial Action at Savannah River Site. *Environ. Sci.*  
822 *Technol.* **2011**, *45* (23), 9975–9983.  
823 (30) Xu, C.; Zhong, J. Y.; Hatcher, P. G.; Zhang, S. J.; Li, H. P.; Ho,  
824 Y. F.; Schwehr, K. A.; Kaplan, D. I.; Roberts, K. A.; Brinkmeyer, R.;  
825 Yeager, C. M.; Santschi, P. H. Molecular environment of stable iodine  
826 and radioiodine (I-129) in natural organic matter: Evidence inferred  
827 from NMR and binding experiments at environmentally relevant  
828 concentrations. *Geochim. Cosmochim. Acta* **2012**, *97*, 166–182.  
829 (31) Kaiser, M.; Kleber, M.; Berhe, A. A. How air-drying and  
830 rewetting modify soil organic matter characteristics: An assessment to  
831

- 832 improve data interpretation and inference. *Soil Biol. Biochem.* **2015**, *80*  
833 (0), 324–340.
- 834 (32) Ryba, S. A.; Burgess, R. M. Effects of sample preparation on the  
835 measurement of organic carbon, hydrogen, nitrogen, sulfur, and  
836 oxygen concentrations in marine sediments. *Chemosphere* **2002**, *48*  
837 (1), 139–147.
- 838 (33) Gillam, A. H.; Lewis, A. G.; Andersen, R. J. Quantitative  
839 determination of hydroxamic acids. *Anal. Chem.* **1981**, *53* (6), 841–  
840 844.
- 841 (34) De La Rosa, J. M.; Gonzalez-Perez, J. A.; Hatcher, P. G.;  
842 Knicker, H.; Gonzalez-Vila, F. J. Determination of refractory organic  
843 matter in marine sediments by chemical oxidation, analytical pyrolysis  
844 and solid-state (13)C nuclear magnetic resonance spectroscopy. *Eur. J.*  
845 *Soil Sci.* **2008**, *59* (3), 430–438.
- 846 (35) Schmidt, M. W. I.; Gleixner, G. Carbon and nitrogen isotope  
847 composition of bulk soils, particle-size fractions and organic material  
848 after treatment with hydrofluoric acid. *Eur. J. Soil Sci.* **2005**, *56* (3),  
849 407–416.
- 850 (36) Otosaka, S.; Schwehr, K. A.; Kaplan, D. I.; Roberts, K. A.;  
851 Zhang, S. J.; Xu, C.; Li, H. P.; Ho, Y. F.; Brinkmeyer, R.; Yeager, C. M.;  
852 Santschi, P. H. Factors controlling mobility of I-127 and I-129 species  
853 in an acidic groundwater plume at the Savannah River Site. *Sci. Total*  
854 *Environ.* **2011**, *409* (19), 3857–3865.
- 855 (37) Kujawinski, E. B.; Hatcher, P. G.; Freitas, M. A. High-Resolution  
856 Fourier Transform Ion Cyclotron Resonance Mass Spectrometry of  
857 Humic and Fulvic Acids: Improvements and Comparisons. *Anal.*  
858 *Chem.* **2002**, *74* (2), 413–419.
- 859 (38) Stubbins, A.; Spencer, R. G. M.; Chen, H.; Hatcher, P. G.;  
860 Mopper, K.; Hernes, P. J.; Mwamba, V. L.; Mangangu, A. M.;  
861 Wabakanghanzi, J. N.; Six, J. Illuminated darkness: Molecular  
862 signatures of Congo River dissolved organic matter and its  
863 photochemical alteration as revealed by ultrahigh precision mass  
864 spectrometry. *Limnol. Oceanogr.* **2010**, *55* (4), 1467–1477.
- 865 (39) Sleighter, R. L.; Hatcher, P. G. Fourier Transform Mass  
866 Spectrometry for the Molecular Level Characterization of Natural  
867 Organic Matter: Instrument Capabilities, Applications, and Limi-  
868 tations. In *Fourier Transforms-Approach to Scientific Principles*; Nikolic,  
869 G., Ed.; InTech: Rijeka, Croatia, 2011.
- 870 (40) Koch, B. P.; Dittmar, T. From mass to structure: an aromaticity  
871 index for high-resolution mass data of natural organic matter. *Rapid*  
872 *Commun. Mass Spectrom.* **2006**, *20* (5), 926–932.
- 873 (41) Haselaw, J. S.; Harris, M. K.; Lonney, B. B.; Halverson, N. V.;  
874 Galdden, J. B. *Analysis of Soil and Water at the Fourmile Branch Seep Line*  
875 *Near the F and H Area of SRS (U)*; Westinghouse Savannah River  
876 Company, Savannah River Technology Center, Savannah River  
877 Laboratory: Aiken, SC, 1990.
- 878 (42) Dai, M.; Buesseler, K. O.; Pike, S. M. Plutonium in groundwater  
879 at the 100K-Area of the U.S. DOE Hanford Site. *J. Contam. Hydrol.*  
880 **2005**, *76* (3–4), 167–189.
- 881 (43) Powell, P. E.; Szaniszlo, P. J.; Reid, C. P. P. Confirmation of  
882 Occurrence of Hydroxamate Siderophores in Soil by a Novel  
883 Escherichia-Coli Bioassay. *Appl. Environ. Microbiol.* **1983**, *46* (5),  
884 1080–1083.
- 885 (44) Powell, P. E.; Cline, G. R.; Reid, C. P. P.; Szaniszlo, P. J.  
886 Occurrence of Hydroxamate Siderophore Iron Chelators in Soils.  
887 *Nature* **1980**, *287* (5785), 833–834.
- 888 (45) Karlsson, T.; Persson, P. Complexes with aquatic organic matter  
889 suppress hydrolysis and precipitation of Fe(III). *Chem. Geol.* **2012**,  
890 *322–323*, 19–27.
- 891 (46) Sjöstedt, C.; Persson, I.; Hesterberg, D.; Kleja, D. B.; Borg, H.;  
892 Gustafsson, J. P. Iron speciation in soft-water lakes and soils as  
893 determined by EXAFS spectroscopy and geochemical modelling.  
894 *Geochim. Cosmochim. Acta* **2013**, *105*, 172–186.
- 895 (47) Sundman, A.; Karlsson, T.; Laudon, H.; Persson, P. XAS study  
896 of iron speciation in soils and waters from a boreal catchment. *Chem.*  
897 *Geol.* **2014**, *364*, 93–102.
- 898 (48) Gu, B.; Schmitt, J.; Chen, Z.; Liang, L.; McCarthy, J. F.  
899 Adsorption and desorption of natural organic matter on iron oxide:  
900 mechanisms and models. *Environ. Sci. Technol.* **1994**, *28* (1), 38–46.
- (49) Neu, M. P.; Matonic, J. H.; Ruggiero, C. E.; Scott, B. L. 901  
Structural characterization of a plutonium(IV) siderophore complex: 902  
Single-crystal structure of Pu-desferrioxamine E. *Angew. Chem., Int. Ed.* 903  
**2000**, *39* (8), 1442–1444. 904
- (50) Chuang, C. Y.; Ho, Y.-F.; Conte, M. H.; Guo, L. D.; Schumann, 905  
D.; Ayranov, M.; Li, Y.-H.; Santschi, P. H. Role of biopolymers as 906  
major carrier phases of Th, Pa, Po, Pb and Be radionuclides in settling 907  
particles from the Atlantic Ocean, in revision. *Mar. Chem.* **2013**, *157*, 908  
131. 909
- (51) Jarvis, N. V.; Hancock, R. D. Some Correlations Involving the 910  
Stability of Complexes of Transuranium Metal-Ions and Ligands with 911  
Negatively Charged Oxygen Donors. *Inorg. Chim. Acta* **1991**, *182* (2), 912  
229–232. 913
- (52) Chen, H. M.; Abdulla, H. A. N.; Sanders, R. L.; Myneni, S. C. B.; 914  
Mopper, K.; Hatcher, P. G. Production of Black Carbon-like and 915  
Aliphatic Molecules from Terrestrial Dissolved Organic Matter in the 916  
Presence of Sunlight and Iron. *Environ. Sci. Technol. Lett.* **2014**, *1* (10), 917  
399–404. 918
- (53) Sleighter, R. L.; Chin, Y.-P.; Arnold, W. A.; Hatcher, P. G.; 919  
McCabe, A. J.; McAdams, B. C.; Wallace, G. C. Evidence of 920  
Incorporation of Abiotic S and N into Prairie Wetland Dissolved 921  
Organic Matter. *Environ. Sci. Technol. Lett.* **2014**, *1* (9), 345–350. 922
- (54) Hertkorn, N.; Benner, R.; Frommberger, M.; Schmitt-Kopplin, 923  
P.; Witt, M.; Kaiser, K.; Kettrup, A.; Hedges, J. I. Characterization of a 924  
major refractory component of marine dissolved organic matter. 925  
*Geochim. Cosmochim. Acta* **2006**, *70* (12), 2990–3010. 926
- (55) Schmidt-Rohr, K.; Mao, J. D.; Olk, D. C. Nitrogen-bonded 927  
aromatics in soil organic matter and their implications for a yield 928  
decline in intensive rice cropping. *Proc. Natl. Acad. Sci. U. S. A.* **2004**, 929  
*101* (17), 6351–6354. 930
- (56) Hartman, M. J.; Morasch, L. F.; Webber, W. D. *Summary of* 931  
*Hanford Site Groundwater Monitoring for Fiscal Year 2002*; PNNL- 932  
14187-SUM; PNNL: Richland, WA, 2003. 933
- (57) Sutton, R.; Sposito, G. Molecular Structure in Soil Humic 934  
Substances: The New View. *Environ. Sci. Technol.* **2005**, *39* (23), 935  
9009–9015. 936
- (58) Ahmed, E.; Holmström, S. J. M. Siderophores in environmental 937  
research: roles and applications. *Microb. Biotechnol.* **2014**, *7* (3), 196– 938  
208. 939
- (59) Powell, R. T.; Wilson-Finelli, A. Photochemical degradation of 940  
organic iron complexing ligands in seawater. *Aquat. Sci.* **2003**, *65* (4), 941  
367–374. 942
- (60) Waggoner, D. C.; Chen, H.; Willoughby, A. S.; Hatcher, P. G. 943  
Formation of black carbon-like and alicyclic aliphatic compounds by 944  
hydroxyl radical initiated degradation of lignin. *Org. Geochem.* **2015**, *82* 945  
(0), 69–76. 946
- (61) Wershaw, R. L. Model for humus in soils and sediments. 947  
*Environ. Sci. Technol.* **1993**, *27* (5), 814–816. 948
- (62) Carrasco, N.; Kretzschmar, R.; Xu, J. D.; Kraemer, S. M. 949  
Adsorption of hydroxamate siderophores and EDTA on goethite in 950  
the presence of the surfactant sodium dodecyl sulfate. *Geochem. Trans.* 951  
**2009**, *10*, 5. 952
- (63) Owen, T.; Butler, A. Metallosurfactants of bioinorganic interest: 953  
Coordination-induced self assembly. *Coord. Chem. Rev.* **2011**, *255* (7– 954  
8), 678–687. 955
- (64) Sutton, R.; Sposito, G. Molecular structure in soil humic 956  
substances: The new view. *Environ. Sci. Technol.* **2005**, *39* (23), 9009– 957  
9015. 958
- (65) Piccolo, A.; Spiteller, M. Electrospray ionization mass 959  
spectrometry of terrestrial humic substances and their size fractions. 960  
*Anal. Bioanal. Chem.* **2003**, *377* (6), 1047–1059. 961
- (66) Piccolo, A. The supramolecular structure of humic substances. 962  
*Soil Sci.* **2001**, *166* (11), 810–832. 963
- (67) Knicker, H. Stabilization of N-compounds in soil and organic- 964  
matter-rich sediments—what is the difference? *Mar. Chem.* **2004**, *92* 965  
(1–4), 167–195. 966
- (68) Kim, S. W.; Kaplan, L. A.; Benner, R.; Hatcher, P. G. Hydrogen- 967  
deficient molecules in natural riverine water samples - evidence for the 968



969 existence of black carbon in DOM. *Mar. Chem.* **2004**, 92 (1–4), 225–  
970 234.